NASA Technical Memorandum 102053
AIAA-89-2805

Numerical Analysis of Supersonic Flow Through Oscillating Cascade Sections by Using a Deforming Grid

Dennis L. Huff
Lewis Research Center
Cleveland, Ohio

and

T.S.R. Reddy
The University of Toledo
Toledo, Ohio

(NASA-TM-102053) NUMERICAL ANALYSIS OF SUPERSONIC FLOW THROUGH OSCILLATING CASCADE SECTIONS BY USING A DEFORMING GRID (NASA. Lewis Research Center) 18 p CSCL 01A

N89-25119

G3/02 Unclas 0216762

Prepared for the
25th Joint Propulsion Conference
cosponsored by the AIAA, ASME, SAE, and ASEE
Monterey, California, July 10-12, 1989

NASA

NUMERICAL ANALYSIS OF SUPERSONIC FLOW THROUGH OSCILLATING CASCADE SECTIONS BY USING A DEFORMING GRID

Dennis L. Huff
National Aeronautics and Space Administration
Lewis Research Center
Cleveland, Ohio 44135

and

T.S.R. Reddy *
The University of Toledo
Toledo, Ohio 43606

Summary

A finite difference code has been developed for modeling inviscid, unsteady supersonic flow by solution of the compressible Euler equations. The code uses a deforming grid technique to capture the motion of the airfoils and can model oscillating cascades with any arbitrary interblade phase angle. A flat plate cascade is analyzed, and results are compared with results from a small-perturbation theory. The results show very good agreement for both the unsteady pressure distributions and the integrated force predictions. The reason for using the numerical Euler code over a small-perturbation theory is the ability to model "real" airfoils that have thickness and camber. Sample predictions are presented for a section of the rotor of a supersonic throughflow compressor designed at NASA Lewis Research Center. Preliminary results indicate that two-dimensional, flat plate analysis predicts conservative flutter boundaries.

Introduction

Recently, there has been interest in designing a turbine engine that operates with supersonic axial flow through the rotor and stator blade rows. Much research is needed to ensure stable operation of this type of design. Understanding the aeroelastic behavior and identifying the flutter boundaries is critical. Many methods used for flutter analysis depend on the successful predictions of blade loading and blade motion. Ideally, this is an interactive process where a structural analysis determines the blade motion from the blade loading and the loading is determined by the flow analysis from the blade motion. Many of the existing structural and aerodynamic analysis methods are based on flat plate theory and introduce approximations to model thickness and camber of the blades. One alternative is to use a finite difference algorithm to predict the flow field and account for these effects.

The present research focuses on numerical solutions of two-dimensional supersonic flow through oscillating cascades. Numerical methods tend to converge faster in this flow regime compared with their subsonic counterparts. The Euler equations are solved instead of the Navier-Stokes equations since the Reynolds numbers for these flows are high. Harmonic pitching motions are prescribed for the blade sections for both zero and nonzero interblade phase angles. The code uses the deforming grid technique introduced in references 1 and 2 for convenient specification of the periodic boundary conditions from blade to blade. Several sample predictions are presented for oscillating cascades in this flow regime. This analysis can be applied to any fan or compressor designs with supersonic relative Mach numbers.

Governing Equations

A major portion of the present code is based on the unsteady solver developed by Sankar and Tang (ref.3) for flow past isolated airfoils. This code solves the two-dimensional, unsteady, Reynolds-averaged, compressible Navier-Stokes equations in strong conservation form on a body-fitted moving coordinate system using an ADI procedure. These equations can be written as

$$\hat{q}_\tau + \hat{F}_\xi + \hat{G}_\eta = \hat{R}_\xi + \hat{S}_\eta \qquad (1)$$

where

$$\hat{q} = J^{-1}\{\rho, \rho u, \rho v, e\} \qquad (2)$$

* NASA Resident Research Associate

and ρ is the fluid density, u and v are the Cartesian components of the fluid velocity, and e is the total energy per unit volume. The body-fitted (ξ, η, τ) coordinate system is related to the Cartesian coordinates by using the following transformation:

$$\begin{aligned} \xi &= \xi(x, y, t) \\ \eta &= \eta(x, y, t) \\ \tau &= t \end{aligned} \tag{3}$$

The Jacobian of the transformation is given by

$$J = \xi_x \eta_y - \eta_x \xi_y = \frac{1}{x_\xi y_\eta - x_\eta y_\xi} \tag{4}$$

and the metrics of the transformation are given by

$$\begin{aligned} \xi_x &= J y_\eta \quad \eta_x = -J y_\xi \\ \xi_y &= -J x_\eta \quad \eta_y = J x_\xi \end{aligned} \tag{5}$$

Standard central differences were used to compute x_ξ, y_ξ, x_η, and y_η which were then used to calculate the metrics.

The $\hat{F}$ and $\hat{G}$ terms in equation (1) are the inviscid terms in the ξ and η-directions, respectively. The viscous terms, $\hat{R}$ and $\hat{S}$, are treated explicitly and can be omitted to give solutions of the Euler equations. In fact, all solutions presented in this paper are inviscid since the Reynolds numbers were relatively high. The Beam-Warming block ADI algorithm is used to solve the governing equations. A Jameson-type artificial dissipation is added in both directions of the computational plane to increase solution stability. The solution is second-order accurate in space and first- or second-order accurate in time. Further information about the algorithm for isolated airfoils can be found in reference 3.

Grid

A unique feature of the present code is the treatment of the grid for oscillating cascades. A method for deforming the grid was developed in references 1 and 2 for zero and nonzero interblade phase angles. The present study uses the same technique.

The code uses a C-grid generated from Sorenson's (ref.4) GRAPE code, which was modified by Chima (ref.5) for improved modeling in turbomachinery problems. One C-grid is generated for each blade in the cascade and undergoes a local deformation associated with the blade motion. The outer boundary of the C-grid is defined by the user in the GRAPE code. A deforming grid technique is used to locate the position of the grid as a function of time. The inner boundary moves with the blade, while the outer boundary remains fixed in space. The grid lines connecting the inner and outer boundaries are allowed to deform. The amount of deformation is a function of the distance away from the surface of the airfoil. A weighting function w is defined as

$$w_{ij} = w(\xi, \eta) = \left| \frac{s(\xi, \eta)}{s(\xi, \eta_{max})} - 1 \right| \tag{6}$$

where s is the arc length of a grid line from the airfoil surface (η=1) to some grid point along ξ = constant, and η_{max} is the outer boundary grid line. The grid deformation is defined as

$$\begin{aligned} \Delta x_{ij} &= w_{ij}(\Delta x'_{ij}) \\ \Delta y_{ij} &= w_{ij}(\Delta y'_{ij}) \end{aligned} \tag{7}$$

where $\Delta x'_{ij}$ and $\Delta y'_{ij}$ are the spatial differences that would exist between successive time steps if the entire grid were moved as a rigid body. From equations (6) and (7), we see that nodes at the inner boundary (s=0) give w_{ij} = 1, which means that the airfoil surface follows the rigid body motion of the blade. Conversely, the outer boundary nodes give w_{ij} = 0, and the node positions remain fixed at the initial specified locations. The interior nodes shear in space relative to the initial grid as w_{ij} varies between 0 and 1. The node velocities can be easily found by dividing the grid deformation by the time step value.

Multiple blade computations are made possible by stacking the C-grids for each blade and passing information between the periodic boundaries. Each C-grid is expanded by one grid line in the η-direction at the outer boundary to provide ghost points for the implementation of the periodic boundary conditions. This allows the periodic boundary condition to be treated implicitly. The zero interblade phase angle is the simplest case for grid generation. Periodic boundary conditions are applied across the upper and lower boundaries and require a grid for only one blade. However, for supersonic axial flow, nonzero interblade phase angles require computations around two additional blades for exact treatment of the periodic boundary conditions. This increases the computational time by a factor of three, but provides an exact boundary condition.

Figure 1 shows a deforming grid for a typical nonzero interblade phase angle computation. Multiblade solutions for oscillating cascades are done by generating grids for each blade and assembling them into a cascade. In this sample case, the interblade phase angle σ is 180 degrees. A 199 by 22 C-grid is generated for a typical section near the midspan of a supersonic throughflow rotor designed at NASA Lewis Research Center. The solver automatically generates the grids for the adjacent blades before the unsteady solution begins by deforming the mean flow grid for one blade through one cycle of oscillation and saving the two grids that occur at the desired interblade phase angle. The grids are then assembled to give the initial multiblade grid to be used for the oscillating cascade solution at $\omega t = 0$ (fig. 1(a)). As time progresses in the unsteady solution, the grid for each blade deforms to model the specified interblade phase angle (fig. 1(b)). Notice how the outer boundary of the grid around each blade remains fixed in space, while the inner boundary follows the motion of the airfoil. An actual run from an oscillating cascade typically has a small pitching amplitude and does not distort the grid as much as shown in figure 1.

Boundary Conditions

The present solution independently solves the flow equations for each grid around a blade and uses periodic boundary conditions along the upper and lower boundaries to model the cascade effects. Ghost points are assigned at the first interior grid line ($\eta = \eta_{max} - 1$) and are used by the adjacent grid from the next blade. Although it is tempting to use the most current flow information as it becomes available from the integration scheme, it is important to only use flow information from the same time step across the periodic boundaries. This eliminates time inaccuracy due to the grid stacking direction of the multiple blade solutions. The metric data are also forced to be continuous along the periodic boundaries. This procedure essentially makes the blade-to-blade periodic boundaries invisible to the flow solution.

In supersonic flow, the domain of the flow field can be reduced by inspecting the shock structures through the cascade. The disturbances generated inside the Mach cone of the leading edge do not influence the flow outside the cone, which means that only three blades need to be considered in the solutions. For example, consider the cascade geometry defined in figure 2, and let the flow conditions be defined such that the bow shock off the leading edge intersects the adjacent blade surfaces. The flow above blade 2 and below blade 3 will have no influence on the surface pressures on blade 1. For this reason, the boundary conditions on the upper and lower boundaries of the global grid (the grid containing all three C-grids) can be arbitrary. The present analysis allows the upper and lower boundaries of the global grid to be periodic, which means that only the surface pressures from the reference blade will be valid for the specified interblade phase angle.

The inlet conditions are assumed to be uniform by specifying the flow density, velocity, flow angle, and pressure. The exit flow variables are extrapolated from the interior by using a simple first-order model. These boundary conditions are valid for supersonic flow at the inlet and exit. Solid wall boundary conditions are applied along the airfoil surface, and the flow variables are averaged across the slit aft of the airfoil.

Results and Discussion

Sample predictions for an oscillating cascade in supersonic flow have been done for both a cascade of flat plates and a midspan section of a proposed rotor design for the supersonic throughflow fan designed at NASA Lewis. There are no unsteady experimental data available for comparisons with the rotor section predictions. At present, any validation of this code is limited to comparisons with a small-perturbation theory for flat plates.

Flat Plate Cascade

Before an unsteady solution can be obtained for an oscillating cascade, a good steady-state solution for the mean flow conditions should be calculated. As previously described, a C-grid is generated for one blade by using a modified GRAPE code. For the present solutions, a 199 by 22 grid in the ξ- and η-directions, respectively, is used around a flat plate with the thickness-to-chord ratio, $\tau = 0.005$. The leading and trailing edges were rounded to aid in C-grid generation, and therefore this is only an approximate representation of a flat plate. Three C-grids are then assembled to define the geometry for the cascade, as shown in figure 3. The present test case was selected from Kielb and Ramsey (ref. 6), who simulated the rotor design for the supersonic throughflow fan by using Lane's theory (ref. 7) to determine the unsteady pressure distributions. The stagger angle γ is 28 degrees and the gap-to-chord ratio g/c is 0.311. An inviscid, steady-state solution has been generated using the present code for $M_1 = 2.61$ and $\beta_1 = 28$ degrees, which gives an incidence angle i of 0 degrees.

Contours of the flow field showing the static pressure are shown in figure 4. The shock structure is clearly defined showing the reflections of the leading edge Mach waves from the surfaces of the adjacent plates. Figure 4(b) shows the detail of the pressure contours near the leading edge of the plates. There is evidence of a bow shock forward of the leading edge, which is expected since the flat plate has finite thickness and will demonstrate blunt body flow characteristics. This will contribute to deviations from theories that use infinitely thin flat plates. Also, there is a slight spreading of the shock waves due to the numerical dissipation inherent to this type of flow code. It is possible to minimize this problem by using a flux vector splitting scheme. In any case, the steady-state solution demonstrates the expected flow characteristics and should provide a reasonable mean flow solution for the oscillating cascade results. The steady-state solution required about 1500 iterations with $\Delta\tau = 0.005$ for the maximum residual to drop four orders of magnitude, which corresponds to about 100 sec of CPU time on the CRAY-YMP. This time can be reduced by implementing a variable local time step instead of the constant time step used in the present solution. Since the focus of the present research is the solution of the unsteady Euler equations, little time has been spent on accelerating the steady-state solutions.

Solutions were done for oscillating flat plates for various interblade phase angles and were compared with the small-perturbation theory of Lane (ref. 7). The unsteady solutions were run with first-order temporal accuracy. The surface pressure time histories were recorded and found to reach a reasonably periodic solution after three cycles of cascade oscillation. A Fourier transform was done on the fourth cycle to determine the first harmonic pressure distribution relative to the airfoil motion. The pressures were normalized by the airfoil pitching amplitude and the phase was referenced to the airfoil pitching motion starting at the maximum (nose-up) blade angle. Predictions for the unsteady pressure difference distributions (ΔCP) on the flat plates are shown in figure 5 for $\sigma = 0$ and 180 degrees, $k = 0.50$, and $\alpha = 0.10$ degrees. The small amplitude of oscillation is used for comparisons with the small-perturbation theory. The agreement with Lane's theory is good for both the real and imaginary parts of pressure, except that the locations of the shock reflections were predicted about 10 percent forward of the Lane's predictions. The actual locations of the shocks are exact for an infinitely thin flat plate, as used by Lane's theory. The finite thickness approximation of the flat plate used in the Euler code is expected to be the greatest contributor to this error. The wiggles near the leading edge of the Euler solution are numerical and are reduced for real airfoils. It is possible to adjust the numerical dissipation coefficients to minimize these wiggles; however the shocks

tend to smear, and the accuracy of the solution becomes jeopardized. The force coefficients obtained by integrating these pressures are insensitive to these wiggles.

In an aeroelastic stability analysis, the moment coefficient about the elastic axis of the blade section can be used for predicting torsional flutter. If the moment coefficient leads the blade motion, the fluid is doing positive work on the blade section and flutter is possible if the blade is perturbed by the prescribed interblade phase angle and if the structural damping cannot control the aerodynamic forces. In the oscillating flat plate cascade presented in this paper, an unstable moment coefficient is predicted for interblade phase angles near 180 degrees. Figure 6 shows how the time history of the moment coefficient lags the blade motion by 81.1 degrees (stable) when $\sigma=0$ and how it leads the plate motion by 151.6 degrees (unstable) when $\sigma=180$ degrees. The moments are calculated about $x'/c=0.30$ (nose-up being positive), which also corresponds to the pitching axes. Note that the first cycle of the solution contains transients from the initialization of the flow field, which was started from uniform flow. A Fourier transform was done on the fourth cycle to determine the harmonic content of moment coefficient. Higher harmonics of the force coefficients were found to be small compared to the fundamental frequency. Figure 7 summarizes the predictions of the imaginary parts of the moment coefficient for various interblade phase angles. When the imaginary part of the moment coefficent becomes positive, the moment leads the motion of the flat plate and represents an unstable condition. Also shown in figure 7 are the predictions using Lane's theory. The agreement is very good over all interblade phase angles in spite of the shock locations being different.

The unsteady solutions use 2.11×10^{-5} sec of CPU per time step per grid point per blade and required 2047 time steps to complete 4.25 cycles of oscillation. In practice, only three cycles of oscillation are necessary to reach a periodic solution, which corresponds to 400 sec of CRAY-YMP CPU time.

Rotor Section Cascade

The reason for using the Euler code over Lane's theory is the ability to model "real" blade sections that have thickness and camber. While Lane's theory offers the most practical analysis tool for investigating a wide range of flutter parameters, the Euler code can be used to check the effects of blade loading. A typical section near the midspan of the rotor on a supersonic throughflow fan design being investigated at NASA Lewis has been chosen for sample unsteady predictions for an oscillating cascade. As in the flat plate results, the steady-state solution is evaluated first to see if the mean flow distribution is reasonable. The parameters for the flow and cascade geometry are similar to those used for the flat plate analysis, except that the airfoils are now loaded to conditions near their design point: $g/c=0.311$, $\gamma=28$ degrees, $M_1=2.61$, and $\beta_1=36.0$ degrees. The grid presented in figure 1 is used in the present investigation and has the same dimensions and parameters described for the grid used in the flat plate analysis. The steady-state predictions for pressure contours and Mach contours are presented in figures 8 and 9, respectively. The pressure contours give a better definition of the shock structure through the cascade. The bow shock, the expansion fan on the upper surface, and the compression shock on the lower surface are all evident near the leading edge, along with their respective reflections from adjacent blades. Also, a weak "fish-tail" shock is formed on the trailing edge. These predictions show all of the expected physics in a supersonic cascade. The addition of thickness and camber to the solution caused the shocks to move forward from their locations in the flat plate analysis, as shown in figure 4.

Two unsteady solutions for the blades oscillating with $\sigma=0$ degrees and 180 degrees, $k=0.50$, and $\alpha=0.1$ degrees are presented in figure 10. The discontinuities near 20- and 70-percent chord are evidence of the shock structures shown in the steady solution. The shock movement due to a pitching amplitude of 0.1 degrees was expectedly small. A stability analysis was done by running the code for various interblade phase angles, as shown in figure 11. The moment coefficients are calculated about a position near the midchord. These results are representative of predictions with the pitching axis at any location along the chord line. The analysis remains stable for all interblade phase angles. In fact, the magnitudes of the imaginary part of the moment coefficients drop by about one order of magnitude when compared with the results from the flat plate analysis in figure 7. The trends from this preliminary analysis suggest that the flat plate analysis of Lane (ref. 7) is conservative for the prediction of flutter. However, this does not show that the rotor design is free of any flutter problems since (1) only one frequency, one Mach number, and one elastic axis were investigated with the Euler code; (2) three-dimensional effects have been neglected; and (3) no structural model has been included. The frequency used in this investigation was chosen as a worst case based on the analysis performed by Kielb and Ramsey (ref. 6). Since the solution in reference 6 used the mean flow from a flat plate analysis, the critical frequency is expected to change for the loaded cascade. Therefore, more frequencies need to be investigated at various Mach numbers to ensure that the design remains stable.

Conclusions

A code has been developed that solves the nonlinear flow field for oscillating cascades in supersonic flow and can be used in flutter analysis. A finite difference code has been developed for modeling compressible, inviscid, unsteady supersonic flow by solution of the Euler equations. The code uses a deforming grid technique to capture the motion of the airfoils and can model oscillating cascades with any arbitrary interblade phase angle. A flat plate analysis is done for comparisons with a small-perturbation theory. The results show very good agreement for both the unsteady pressure distributions and the integrated force predictions. Sample predictions are presented for a section of the rotor on a supersonic throughflow compressor designed at NASA Lewis Research Center. Preliminary results indicate that two-dimensional, flat plate analysis predicts conservative flutter boundaries.

The code is a tool for modeling "real" blade sections, which can have significantly different flow characteristics than results from methods that are restricted to flat plate geometries. Obviously, further research is needed to validate the code, such as detailed experimental data for oscillating cascades. It is possible to add a simple two-dimensional structural model to evaluate the effects of structural properties. Also, an extension to the three-dimensional flow equations may be needed to better model the actual compressor design.

Appendix - Symbols

C	sonic velocity
CM	moment coefficient
CP	pressure coefficient, $\frac{p-p_1}{\rho_1 V_1^2}$
c	blade chord length
e	total energy of the fluid per unit volume
g/c	gap-to-chord ratio
$\mathcal{Im}\{\ \}$	imaginary part of { }
i	incidence angle
J	Jacobian of transformation
k	reduced frequency based on semichord, $\frac{\omega c}{2V_1}$
M	Mach number
Re	Reynolds number based on chord
$\mathcal{Re}\{\ \}$	real part of { }
s	arc length of a grid line in the η-direction
t	time normalized by $\frac{c}{C_1}$
u, v	Cartesian velocities normalized by C_1
V	total velocity
w	weighting function for grid deformation
x', y'	Cartesian coordinates
α	amplitude of pitching
β	flow angle
γ	stagger angle
ΔCP	pressure difference coefficient, $CP_- - CP_+$
η	normal direction of transformed coordinate system
ξ	chordwise direction of transformed coordinate system
ρ	fluid density
σ	interblade phase angle
τ	time variable
τ'	thickness-to-chord ratio
ω	airfoil oscillation frequency

Subscripts:

1	conditions at the inlet
2	conditions at the exit
+,-	upper and lower surfaces on airfoil, respectively

References

1. Huff, D.L., "Numerical Simulations of Unsteady, Viscous, Transonic Flow Over Isolated and Cascaded Airfoils Using a Deforming Grid," AIAA Paper 87-1316, June 1987. (Also, NASA TM-89890.)

2. Huff, D.L., "Numerical Analysis of Flow Through Oscillating Cascade Sections," AIAA Paper 89-0437, Jan. 1989. (Also, NASA TM-101417.)

3. Sankar, N.L. and Tang, W., "Numerical Solution of Unsteady Viscous Flow Past Rotor Sections," AIAA Paper 85-0129, Jan. 1985.

4. Sorenson, R.L., "A Computer Program to Generate Two-Dimensional Grids About Airfoils and Other Shapes by the Use of the Poisson's Equations," NASA TM-81198, 1980.

5. Chima, R.V., "Explicit Multigrid Algorithm for Quasi-Three-Dimensional Viscous Flow in Turbomachinery," Journal of Propulsion and Power, Vol. 3, No. 5, Sept.-Oct. 1987, pp. 397-405.

6. Kielb, R.E. and Ramsey, J.K., "Flutter of a Fan Blade in Supersonic Axial Flow," ASME Paper 88-GT-78, June 1988.

7. Lane, F., "Supersonic Flow Past an Oscillating Cascade with Supersonic Leading-Edge Locus," Journal of the Aeronautical Sciences, Vol. 24, No. 1, Jan. 1957, pp. 65-66.

ORIGINAL PAGE IS
OF POOR QUALITY

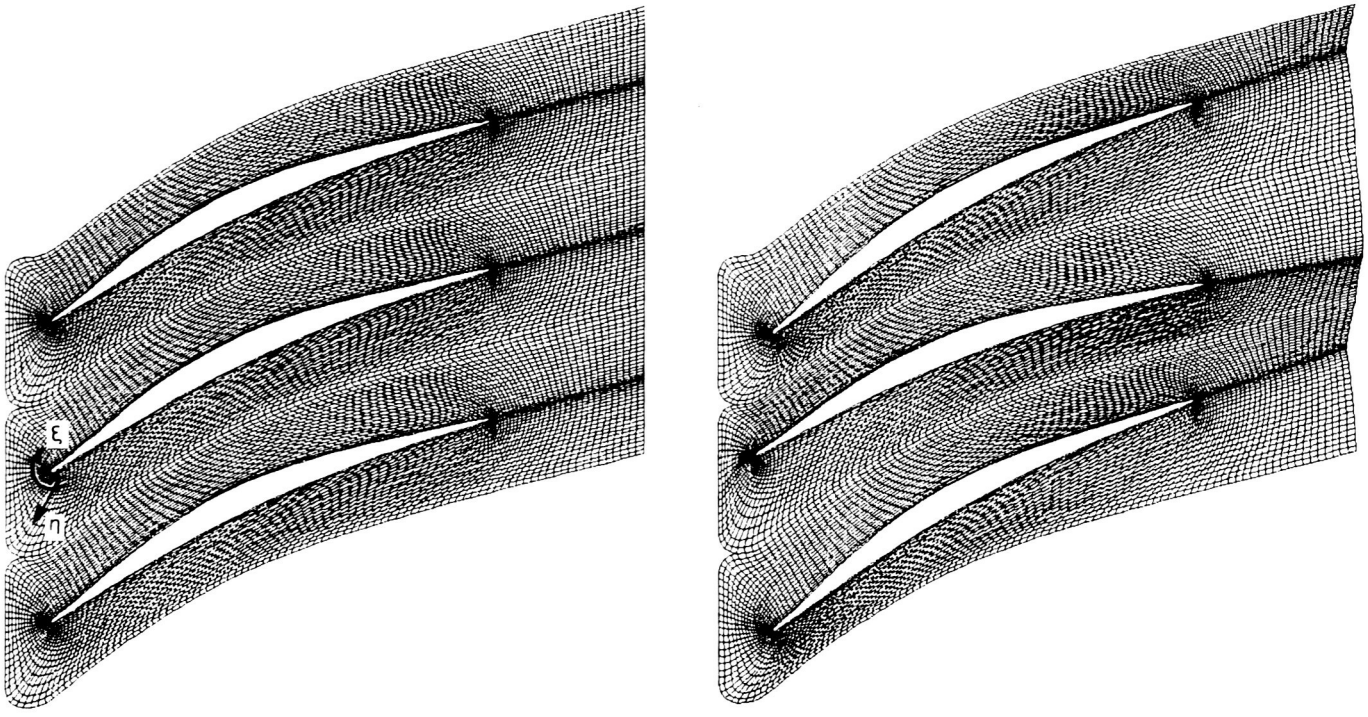

(a) $\omega t = 0°$.

(b) $\omega t = 90°$.

Figure 1.—Deforming grid technique with exaggerated motion.

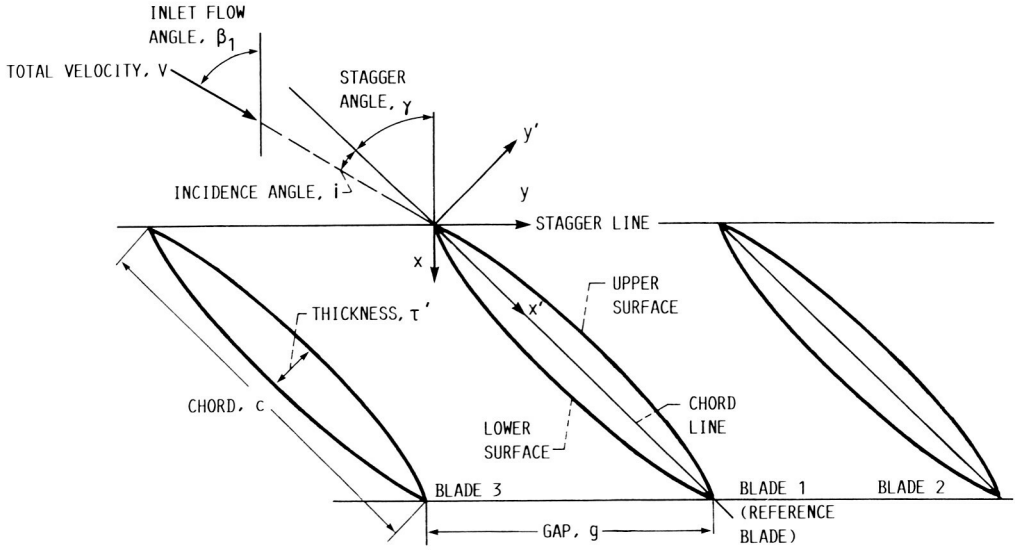

Figure 2.—Cascade geometry.

ORIGINAL PAGE IS
OF POOR QUALITY

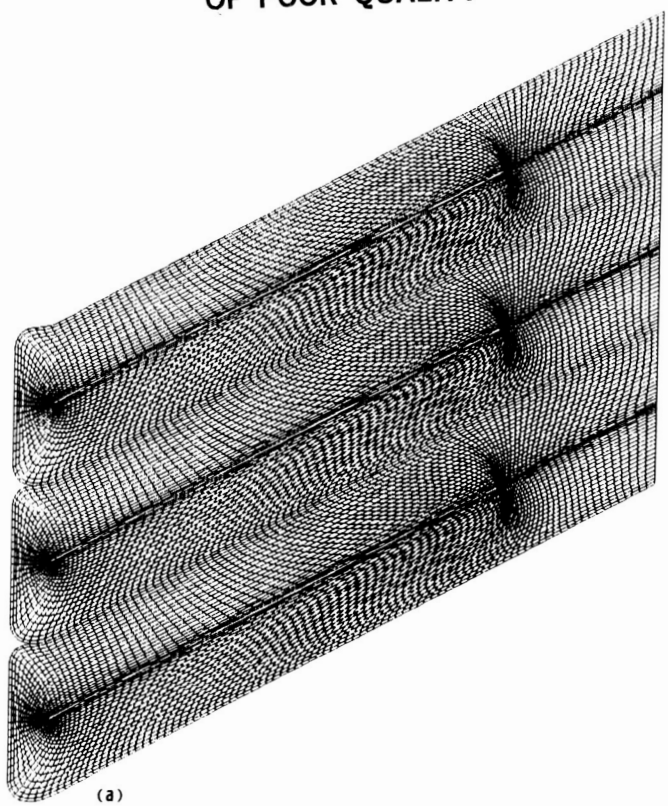

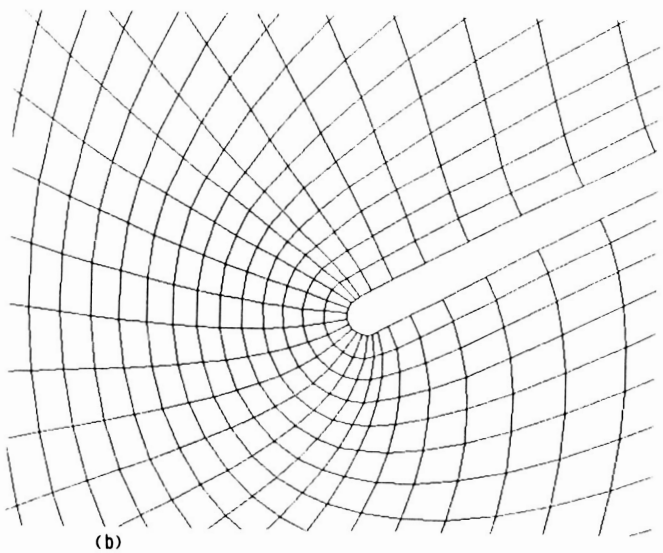

(a) Global grid.
(b) Enlarged view of leading-edge region.

Figure 3.—Grid for flat plate cascade.

ORIGINAL PAGE
COLOR PHOTOGRAPH

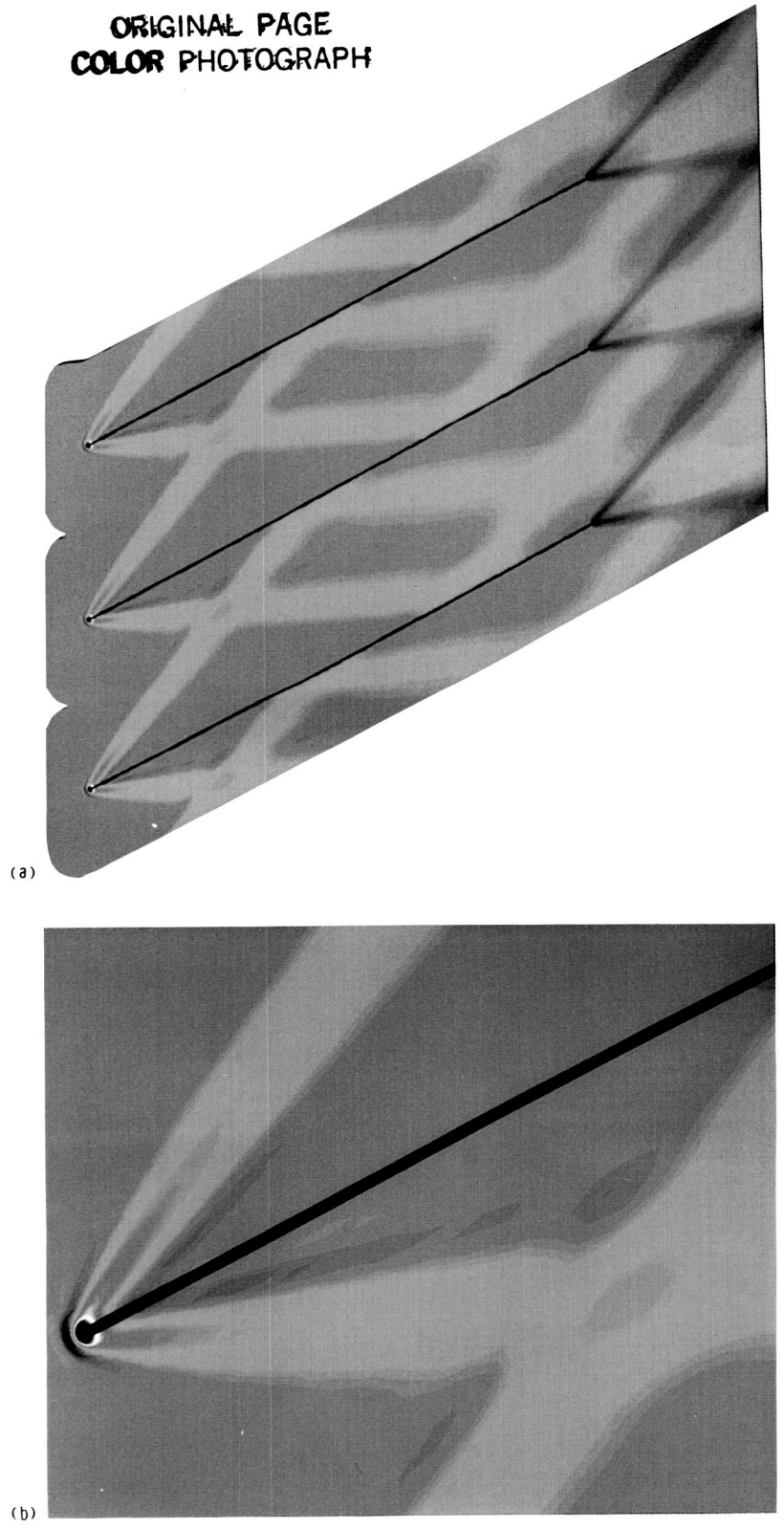

(a) Global grid.
(b) Enlarged view of leading-edge region.

Figure 4.—Static pressure contours for flat plate cascade. Inlet Mach number, M_1, 2.61; stagger angle, γ, 28°; gap-to-chord ratio, g/c, 0.311; inlet flow angle, β_1, 28° (incidence angle, i, 0°), thickness-to-chord ratio, τ', 0.005. Blue indicates lower pressure; red indicates higher pressure.

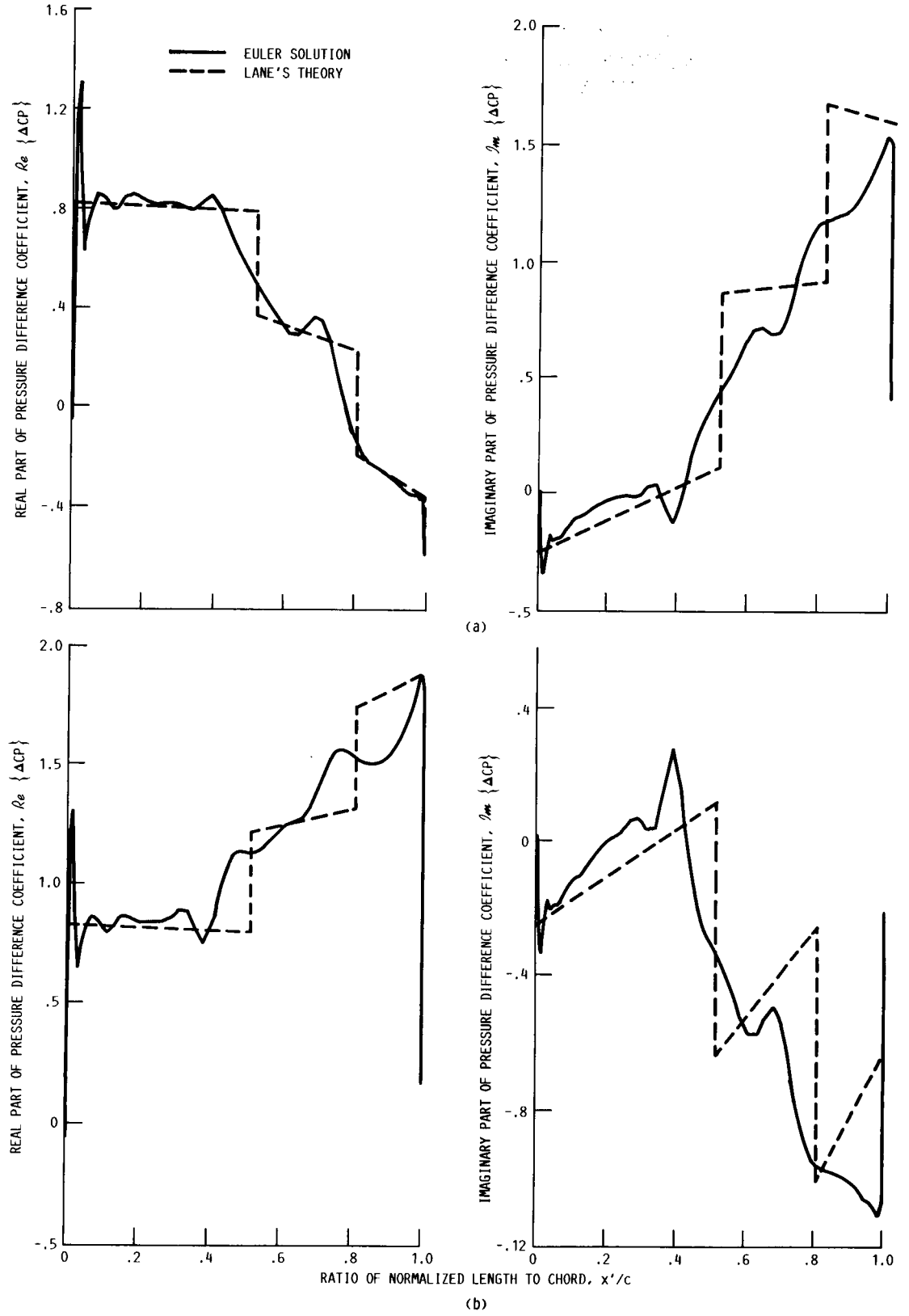

(a) Interblade phase angle, σ, 0°.
(b) Interblade phase angle, σ, 180°.

Figure 5.—First harmonic pressure difference distribution for flat plate cascade. Stagger angle, γ, 28°; gap-to-chord ratio, g/c, 0.311; inlet flow angle, β_1, 28°±0.10°; reduced frequency based on semichord, k, 0.5.

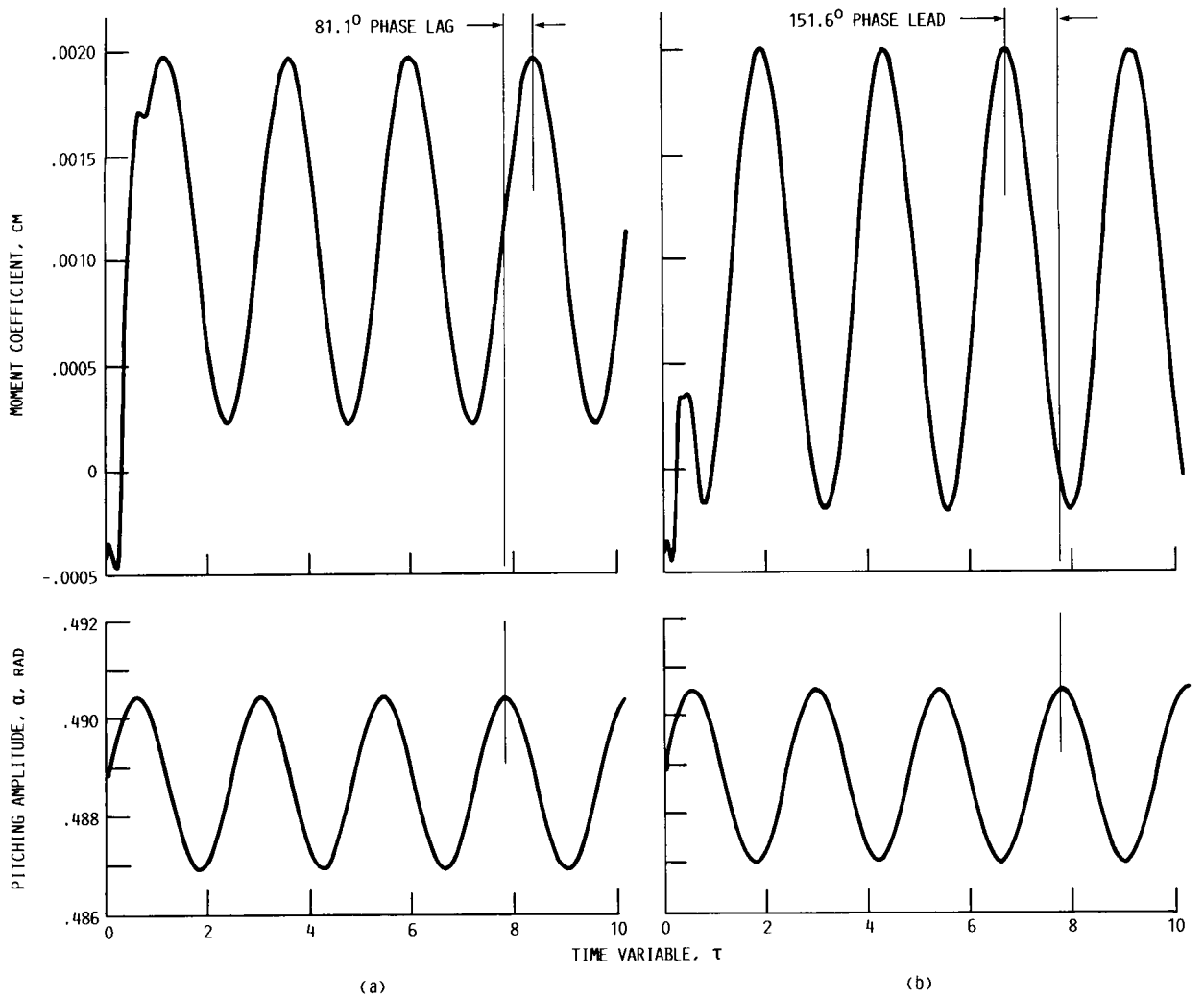

(a) Interblade phase angle, σ, 0°.
(b) Interblade phase angle, σ, 180°.

Figure 6.—Time history of moment coefficient about x′/c = 0.30; flat plate cascade. Inlet Mach number, M_1, 2.61; stagger angle, γ, 28°; gap-to-chord ratio, g/c, 0.311; inlet flow angle, β_1, 28°±0.10°; reduced frequency based on semichord, k, 0.5.

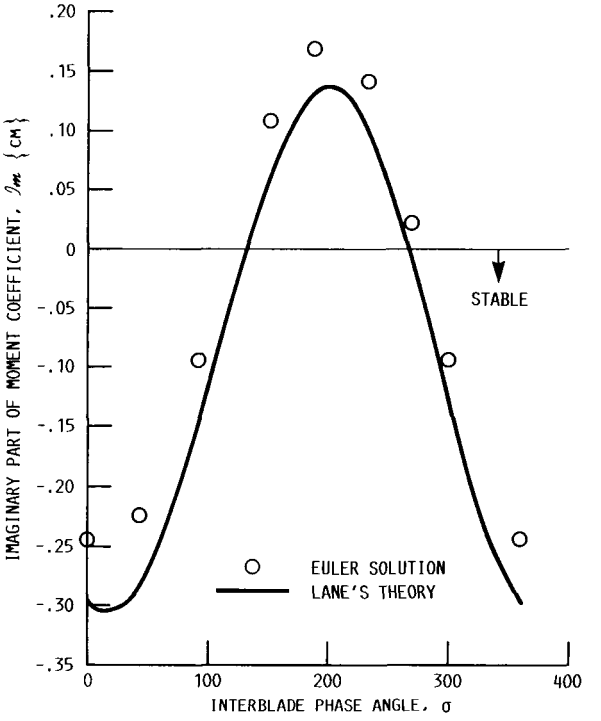

Figure 7.—Imaginary part of moment coefficient about $x'/c = 0.30$ versus interblade phase angle; flat plate cascade. Inlet Mach number, M_1, 2.61; stagger angle, γ, 28; gap-to-chord ratio, g/c, 0.311; inlet flow angle, β_1, $28° \pm 0.10°$; reduced frequency based on semichord, k, 0.5.

ORIGINAL PAGE
COLOR PHOTOGRAPH

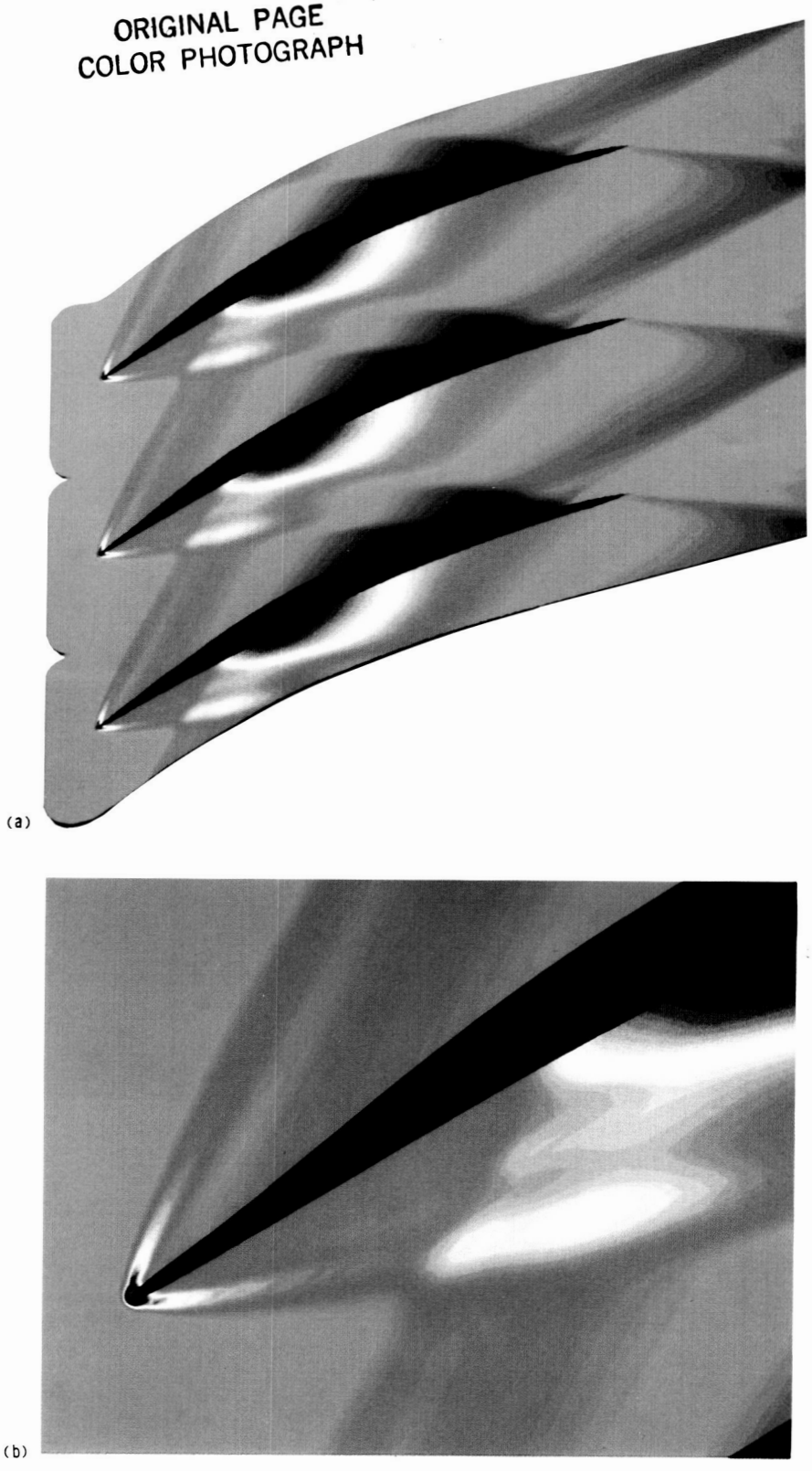

(a) Global grid.
(b) Enlarged view of leading-edge region.

Figure 8.—Static pressure contours for rotor cascade. Inlet Mach number, M_1, 2.61; stagger angle, γ, 28°; gap-to-chord ratio, g/c, 0.311; inlet flow angle, β_1, 36°. Blue indicates lower pressure; red indicates higher pressure.

ORIGINAL PAGE
COLOR PHOTOGRAPH

ORIGINAL PAGE
COLOR PHOTOGRAPH

Figure 9.—Mach number contours for rotor cascade. Inlet Mach number, M_1, 2.61; stagger angle, γ, 28°; gap-to-chord ratio, g/c, 0.311; inlet flow angle, β_1, 36°. Yellow indicates lower Mach number; pink indicates higher Mach number.

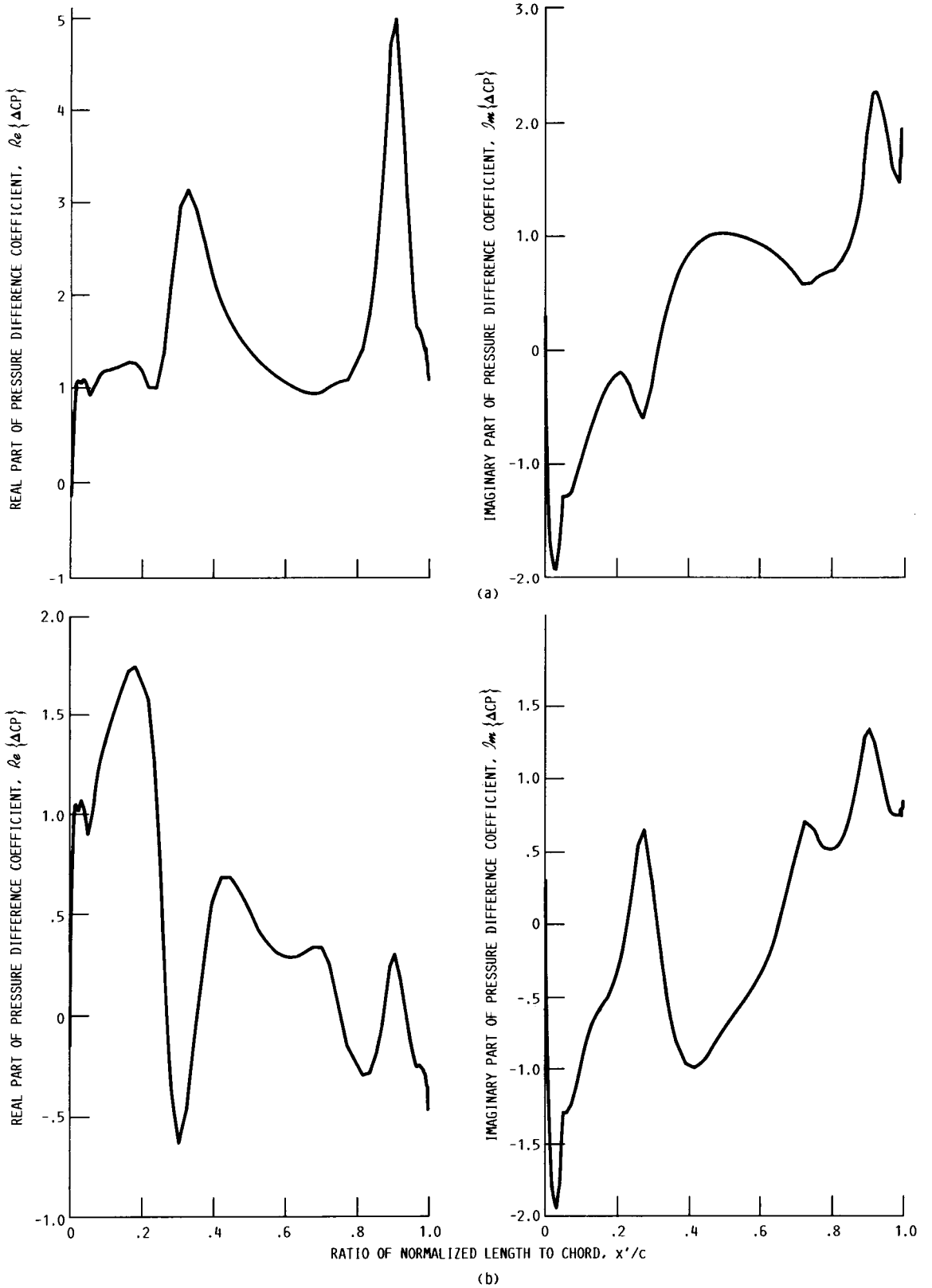

(a) Interblade phase angle, σ, 0°.
(b) Interblade phase angle, σ, 180°.

Figure 10.—First harmonic pressure difference distribution for rotor cascade. Inlet Mach number, M_1, 2.61; stagger angle, γ, 28°; gap-to-chord ratio, g/c, 0.311; inlet flow angle, β_1, 36°±0.10°; reduced frequency based on semichord, k, 0.5.

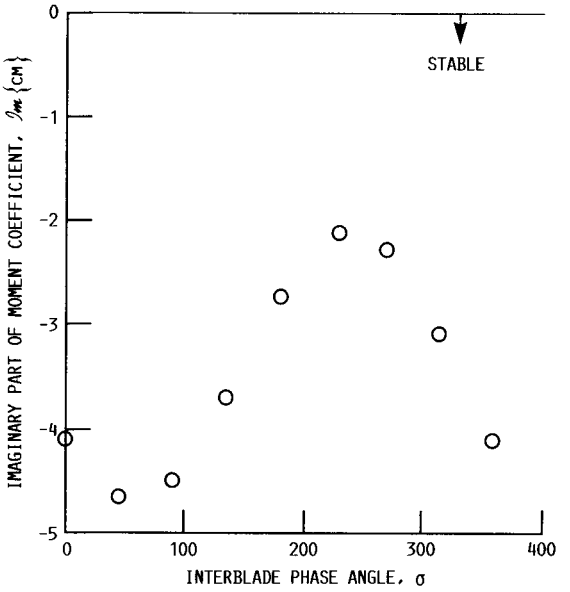

Figure 11.—Imaginary part of moment coefficient near midchord versus interblade phase angle; rotor cascade. Inlet Mach number, M_1, 2.61; stagger angle, γ, 28; gap-to-chord ratio, g/c, 0.311; inlet flow angle, β_1, 36°±0.10°; reduced frequency based on semichord, k, 0.5.

NASA
National Aeronautics and Space Administration

Report Documentation Page

1. Report No.	2. Government Accession No.	3. Recipient's Catalog No.
NASA TM-102053 AIAA-89-2805		

4. Title and Subtitle

Numerical Analysis of Supersonic Flow Through Oscillating Cascade Sections by Using a Deforming Grid

5. Report Date

6. Performing Organization Code

7. Author(s)

Dennis L. Huff and T.S.R. Reddy

8. Performing Organization Report No.

E-4805

10. Work Unit No.

535-03-01

9. Performing Organization Name and Address

National Aeronautics and Space Administration
Lewis Research Center
Cleveland, Ohio 44135-3191

11. Contract or Grant No.

13. Type of Report and Period Covered

Technical Memorandum

12. Sponsoring Agency Name and Address

National Aeronautics and Space Administration
Washington, D.C. 20546-0001

14. Sponsoring Agency Code

15. Supplementary Notes

Prepared for the 25th Joint Propulsion Conference cosponsored by the AIAA, ASME, SAE, and ASEE, Monterey, California, July 10-12, 1989. Dennis L. Huff, NASA Lewis Research Center; T.S.R. Reddy, The University of Toledo, Toledo, Ohio 43606 and NASA Resident Research Associate.

16. Abstract

A finite difference code has been developed for modeling inviscid, unsteady supersonic flow by solution of the compressible Euler equations. The code uses a deforming grid technique to capture the motion of the airfoils and can model oscillating cascades with any arbitrary interblade phase angle. A flat plate cascade is analyzed, and results are compared with results from a small-perturbation theory. The results show very good agreement for both the unsteady pressure distributions and the integrated force predictions. The reason for using the numerical Euler code over a small-perturbation theory is the ability to model "real" airfoils that have thickness and camber. Sample predictions are presented for a section of the rotor on a supersonic throughflow compressor designed at NASA Lewis Research Center. Preliminary results indicate that two-dimensional, flat plate analysis predicts conservative flutter boundaries.

17. Key Words (Suggested by Author(s))	18. Distribution Statement
Oscillating cascades; Supersonic flow; Turbomachinery; Euler equations; Numerical analysis	Unclassified – Unlimited Subject Category 02

19. Security Classif. (of this report)	20. Security Classif. (of this page)	21. No of pages	22. Price*
Unclassified	Unclassified	18	A03

*For sale by the National Technical Information Service, Springfield, Virginia 22161